J. Cell. Mol. Med. Vol 14, No 6B, 2010 pp. 1605-1618

Human liver stem cell-derived microvesicles accelerate hepatic regeneration in hepatectomized rats

M. B. Herrera [a, e, #], V. Fonsato [a, #], S. Gatti [b, #], M. C. Deregibus [a], A. Sordi [b], D. Cantarella [c], R. Calogero [c], B. Bussolati [a], C. Tetta [e, d], G. Camussi [a, *]

[a] Department of Internal Medicine, Research Center for Experimental Medicine (CeRMS), and Center for Molecular Biotechnology, Torino, Italy
[b] Center for Surgical Research, Fondazione IRCCS Ospedale Maggiore Policlinico, Mangiagalli e Regina Elena, Milano, Italy
[c] Department of Clinical and Biological Sciences, University of Torino, Torino, Italy
[d] Fresenius Medical Care, Bad Homburg, Germany
[e] Sister Spa, Palazzo Pignano, Italy

Received: April 17, 2009; Accepted: July 10, 2009

Abstract

Several studies indicate that adult stem cells may improve the recovery from acute tissue injury. It has been suggested that they may contribute to tissue regeneration by the release of paracrine factors promoting proliferation of tissue resident cells. However, the factors involved remain unknown. In the present study we found that microvesicles (MVs) derived from human liver stem cells (HLSC) induced *in vitro* proliferation and apoptosis resistance of human and rat hepatocytes. These effects required internalization of MVs in the hepatocytes by an α_4-integrin-dependent mechanism. However, MVs pre-treated with RNase, even if internalized, were unable to induce hepatocyte proliferation and apoptosis resistance, suggesting an RNA-dependent effect. Microarray analysis and quantitative RT-PCR demonstrated that MVs were shuttling a specific subset of cellular mRNA, such as mRNA associated in the control of transcription, translation, proliferation and apoptosis. When administered *in vivo*, MVs accelerated the morphological and functional recovery of liver in a model of 70% hepatectomy in rats. This effect was associated with increase in hepatocyte proliferation and was abolished by RNase pre-treatment of MVs. Using human AGO2, as a reporter gene present in MVs, we found the expression of human AGO2 mRNA and protein in the liver of hepatectomized rats treated with MVs. These data suggested a translation of the MV shuttled mRNA into hepatocytes of treated rats. In conclusion, these results suggest that MVs derived from HLSC may activate a proliferative program in remnant hepatocytes after hepatectomy by a horizontal transfer of specific mRNA subsets.

Keywords: stem cells • microvesicles • hepatectomy • liver regeneration

Introduction

Several reports suggest that the administration of *in vitro* expanded stem cells might promote liver regeneration [1, 2]. Sources of pluripotent cells with hepatic potential include adipose tissue [3], bone marrow derived-stem cells [4–6] and embryonic stem cells [7]. However, the mechanisms involved in hepatic regeneration are not completely understood and the relative contribution of mature hepatocytes and of resident stem cells is still intensely debated [8]. It has been suggested that bone marrow derived stem cells may engraft in the liver undergoing transdifferentiation or fusion [9–11]. However, more recent studies have suggested that tissue regeneration triggered by exogenous stem cells may depend on the release of paracrine factors rather than on stem cell transdifferentiation [12–15]. The liver is known to have the capacity to regenerate after injury induced by chemicals, partial surgical resection or sepsis [8, 16]. Following partial hepatectomy, most of the quiescent hepatocytes in the remnant liver tissue quickly proliferate leading to rapid restoration of liver mass [17]. Whether resident stem cells are involved in such regeneration remains unknown. We recently described in the adult human liver a population of pluripotent resident liver stem cells (HLSC) able to localize within the injured liver and contribute to liver regeneration

# These authors contributed equally.
*Correspondence to: Giovanni CAMUSSI,
Dipartimento di Medicina Interna,
Ospedale Maggiore S. Giovanni Battista,
Corso Dogliotti 14, 10126, Torino, Italy.
Tel.: +39-011-6336708
Fax: +39-011-6631184
E-mail: giovanni.camussi@unito.it

doi:10.1111/j.1582-4934.2009.00860.x

when injected in mice with acute liver failure induced by acetoaminophene [18]. Recently, it has been proposed that a dynamic stem cell regulation may occur as result of differentiated cell-stem cell interaction *via* a microvesicle (MV)-based genetic information transfer [19]. Progenitor/stem cells may re-direct the behaviour of differentiated cells by a horizontal transfer of mRNA shuttled by MVs [20, 21] and conversely differentiated cells may influence the stem cell phenotype [19]. MVs are derived from the endosomal membrane compartment after fusion with the plasma membrane and are shed from the cell surface of activated cells. MVs are now recognized to have an important role in cell to cell communication [22]. Ratajczak and coworkers [20] demonstrated that MVs derived from embryonic stem cells may contribute to the cell-fate decision and may represent one of the critical components that support self-renewal and expansion of stem cells. We demonstrated that MVs derived from endothelial progenitor cells may activate an angiogenic program in mature quiescent endothelial cells [21] and that mRNA shuttled by MVs derived from mesenchymal stem cells may induce repair of acute kidney injury [23]. Recently Kostin and Popescu [24] demonstrated that the interstitial Cajal-like cells that have been described to be present in the heart [25], communicate with neighbouring cells *via* shedding of MVs.

In the present study we characterized the MVs derived from HLSC and their potential to induce proliferation and apoptosis resistance in cultured human hepatocytes and to favour liver regeneration in the model of 70% hepatectomy in rats.

Materials and methods

Isolation and characterization of HLSC

HLSC were isolated from human cryopreserved normal adult hepatocytes (Lonza, Basel, Switzerland). The isolation, culture and characterization of HLSC were performed as previously described [18]. By cytofluorimetric analysis HLSC expressed the mesenchymal stem cell markers CD29, CD44, CD73, CD90 but not the haematopoietic and endothelial markers CD34, -CD45, -CD14, -CD117, -CD133, -CD31, -CD144. Moreover, HLSC were positive for α_5-integrin, α_4-integrin, α_6-integrin and -$\alpha v\beta_3$-integrin. By immunofluorescence HLSC were positive for the hepatic markers human albumin and α-fetoprotein, for the resident stem cells markers vimentin and nestin and were negative for the oval cell markers CD34, CD117 and cytocheratin19 [18]. In addition, HLSC expressed the embryonic stem cell markers nanog, Oct4, SOX2 and SSEA4. Before use HLSC were shown to undergo osteogenic, endothelial and hepatic differentiation under appropriate culture conditions [18].

Isolation of MVs

MVs were obtained from supernatants of HLSC cultured overnight in α-MEM deprived of foetal calf serum (FCS). The viability of HLSC at the time of MV collection was >99% as detected by trypan blue exclusion. After centrifugation at 2000 $\times$ *g* for 20 min. cell-free supernatants were ultracentrifuged at 100,000 $\times$ *g* (Beckman Coulter Optima L-90K, Optima L-90K, Beckman Coulter, Fullerton, CA, USA) for 1 hr at 4°C, washed in serum-free medium 199 containing Hepes 25 mM (Sigma, St. Louis, MO, USA) and submitted to a second ultracentrifugation in the same conditions [21, 23]. The protein content of MV preparation was quantified by Bradford method (Bio-Rad, Hercules, CA, USA). To trace MVs by fluorescent microscopy or cytofluorimetry, MVs were labelled with the red fluorescent aliphatic chromophore PKH26 (Sigma) [23]. Endotoxin contamination of MVs was excluded by Limulus test (Charles River Laboratories, Inc., Wilmington, MA, USA).

In selected experiments MVs from HLSC were treated with 1 U/ml RNase (Ambion, Inc., Austin, TX, USA) [21, 23] for 1 hr at 37°C, the reaction was stopped by addition of 10 U/ml RNase inhibitor (Ambion) followed by ultracentrifugation. The effectiveness of RNase treatment was evaluated as previously described [23] by spectrophotometer analysis of total extracted RNA (untreated: 4.1 $\pm$ 0.3 μg RNA/mg protein MVs; RNase treated: <0.2 μg RNA/mg protein MVs). As control, MVs were treated with 1 U/ml DNase (Ambion) for 1 hr at 37°C.

Cytofluorimetric analysis of MVs

The size of MVs was determined by cytofluorimetry as previously described [21, 23] using beads of different sizes (1, 2 and 4 μm; Molecular Probes, Leiden, The Netherlands). The analysis was performed using a log scale for forward scatter and side scatter parameters. Moreover, the size of MVs, was evaluated by the Zetasizer Nano (Malvern Instruments, Malvern Worcestershire, UK). Cytofluorimetric analysis for the detection of surface molecules was performed as previously described [21, 23], using the following FITC- or PE-conjugated antibodies directed to: CD44 (Dakocytomation, Copenhagen, Denmark), CD29, α4-integrin, (BD Pharmingen), α5-integrin, α6-integrin (BioLegend, San Diego, CA, USA) and HLA-I (BD Pharmingen). FITC or PE mouse nonimmune isotypic IgG (Dakocytomation, Copenhagen, Denmark) were used as control.

Culture of hepatocytes

Human hepatocytes (Lonza) were cultured in William's medium supplemented with 10% of FCS, 7.5 μg/ml hydrocortisone, 200 μg/ml streptomycin and 200 U/ml penicillin. Rat hepatocytes were obtained from liver of healthy male Sprague–Dawley rats using a two-step collagenase perfusion procedure and were cultured as previously described [26]. Cell viability was greater than 90% as determined by trypan blue exclusion.

Incorporation of MVs in hepatocytes

To study the incorporation of MVs into hepatocytes, we incubated 50 μg/ml of MVs labelled with PKH-26 dye for 3 hrs at 37°C. We studied the MV incorporation by cytofluorimetry and confocal microscopy (LSM 5 Pascal Confocal Microscope, Carl Zeiss International, Oberkochen, Germany).

To investigate the role of adhesion molecules expressed by MVs in the incorporation in hepatocytes, MVs were pre-incubated (15 min. at 4°C) with blocking antibodies (1 μg/ml) against the identified adhesion molecules anti-α_4-integrin (Biolegend), α_6-integrin (Biolegend), CD29 (β_1- integrin) (BD Pharmingen) or with soluble hyaluronic acid (sHA) (100 μg/ml from Rooster comb; Sigma) before the incubation with the cells. In selected experiments labelled MVs were treated with 0.5 mM

trypsin for 30 min. at 37°C and the integrity of MVs and removal of surface molecules was checked by cytofluorimetric analysis.

Cell proliferation and apoptosis

Hepatocyte were seeded at 50,000 cells/well into 48-well plates in William's medium E (Gibco, Paisley, UK) deprived of FCS. DNA synthesis was detected as incorporation of 5-bromo-2′-deoxy-uridine (BrdU) into the cellular DNA after 48 hrs of culture. This time point was chosen on the base of preliminary comparative experiments with [3H] thymidine incorporation. Cells were then fixed with 0.5 M ethanol/HCl and incubated with nuclease to digest the DNA. BrdU incorporated into the DNA was detected using an anti-BrdU peroxidise conjugated antibody (Roche Applied Science, Mannheim, Germany). Optical density was measured with an ELISA reader at 405 nm.

Apoptosis was evaluated by terminal deoxynucleotidyl transferase-mediated dUTP nick-end labelling (TUNEL) technology (Chemicon, CA, USA) as previously described [27]. To induce apoptosis hepatocytes were incubated with 5 mM of D-galactosamine (GalN) for 24 hrs in DMEM supplemented with 2% FCS [28]. Apoptosis was also evaluated in paraffin-embedded liver sections by TUNEL.

Gene array analysis

RNA extraction, samples labelling and hybridization on BeadChips

RNA was extracted from MVs using TRIZOL reagent (Invitrogen, Paisley, UK) following the procedure suggested by the manufacturer. Total RNA was quantified spectrophotometrically (Nanodrop ND-1000, Wilmington DE, USA). cRNA was synthesized using three different quantities of total RNA (0.25, 0.5 and 1 μg). cRNA synthesis and labelling was done using Illumina RNA Amplification Kit (Ambion) following the procedure suggested by manufacturer. Sentrix® Human-6 Expression BeadChip hybridization, washing and staining were also done as suggested by the manufacturer. Arrays were scanned on Illumina BeadStation 500 (Illumina, San Diego, CA, USA).

Microarray data analysis

BeadChip array data quality control was performed with Illumina BeadStudio software version 3.0. Transcript average intensity signals were calculated with BeadStudio without background correction. Raw data were analysed using Bioconductor [29]. Average transcript intensities were log2 transformed and normalized by loess method [30].

A simple statistical linear model [21] was used to identify transcript signals linearly correlated to the increment of total RNA concentration used to prepare cRNA. In equation (1) y_{ij} is the observed expression level for transcript i in sample j ($j = 1, \ldots, 6$). μ is the average expression level of transcript i and β_{RNA} represents the effect of total RNA concentration on the expression level of transcript i. ε represents random error for transcript i and sample j, and it is assumed to be independent for each transcript and sample, and normally distributed with mean 0 and variance σ^2.

$$y_{ij} = \mu + \beta_{RNA} + \varepsilon_{ij}$$

Transcripts characterized by a model with $P \leq 0.05$, $r^2 \geq 0.8$, and a positive slope were selected (120; see additional information 1).

Transcripts annotation and data mining were performed with IPA 7.0 software (www.ingenuity.com). Microarray data were deposited on GEO database (http://www.ncbi.nlm.nih.gov/projects/geo/) as geo accession GSE15569.

Quantitative real time polymerase chain reaction (Q-PCR)

Q-PCR was performed as previously described [31] on four different MV preparations and on livers of Sprague–Dawley rats treated with MVs. Cell cDNA was used to evaluate primers efficiency. The primers for the human genes used for real time PCR were: (*AGO2*; forward 5′ CTAGACCCGACTTTGGGACCT-3′, reverse 5′-GGGCACTTCTCTGGCTTGATA-3; *CHECK2*; forward 5′-AGAAAGCTCTGGACCTTGTCAAGA-3′, reverse 5′-TGGATTCATTTTCCTCAGACAGAA-3′; *CDK2*; forward 5′-AATCCGCCTGGACACTGAGA -3′, reverse 5′-TCCAGCAGCTTGACAATATTAGGA-3′, *MATK* forward 5′-CCGCGACGTCATCCACTAC-3′, reverse 5′-TGTAATGCTCCACCATGTCCAT-3′ and the primers for the rat CCNA1 gene were: forward primer 5′-AAGTCCTGGCATTCGATCTGA-3′, reverse primer 5′-TGCAACATACTTGGCCAAATT-3′. First-strand cDNA was produced from 200 ng of mRNA using High Capacity cDNA Reverse Transcription Kit (Applied Biosystems, Foster City, CA, USA). 20 μl of RT-PCR mix, containing 1× SYBR GREEN PCR Master Mix (Applied Biosystems), 200 nM of each primer and, respectively, 1 μl of MV cDNA, were assembled using a 48-wells StepOneTM Real Time System (Applied Biosystems). Negative cDNA controls (no cDNA) were cycled in parallel with each run.

RT-PCR

Total RNA extracted from livers of rats was submitted to RT-PCR using the following primer for human AGO2 forward 5′ CTAGACCCGACTTTGGGACCT-3′ and reverse 5′-GGGCACTTCTCTGGCTTGATA-3. Bands of the expected size (90 pb) were detected in a 4% agarose gel after electrophoresis. cDNA from a preparation of HLSC was used as positive control.

Immunoprecipitation and Western blot

Rat liver tissue was homogenized (TissueRuptor, Qiagen, Valencia, CA, USA). Proteins were lysated with 1 μl of lysis buffer containing 25 mM Tris•HCl pH 7.6, 150 mM NaCl, 1% NP-40, 1% sodium deoxycholate, 0.1% SDS, 1 mM PMSF, protease and phosphatase inhibitor cocktails (all from Sigma) as previously described [27]. The lysates after pre-clearing with protein A–coupled Sepharose (Amersham, Buckinghamshire, UK) were incubated with human anti-AGO2 antibody (Abcam, Cambridge, MA, USA) overnight at 4°C, under agitation. Samples were subjected to SDS-PAGE in 8% acrylamide gel and transferred to a nitrocellulose membrane as described [27]. Membrane was revealed with a chemiluminescence reagent and analysed with Chemidoc (Biorad, Hercules, CA, USA). Western blot was also performed on MV lysates for detection of Staufen 2 using 8–16% linear gradient acrylamide gels (Biorad) and anti-STAU2 mouse monoclonal antibody (Abcam).

Rat model of 70% hepatectomy

All experiments were performed in accordance with the Principles of Laboratory Animal Care and approved by the Local Committee for Experimental Animal Research. Adult Sprague–Dawley rats (Charles River,

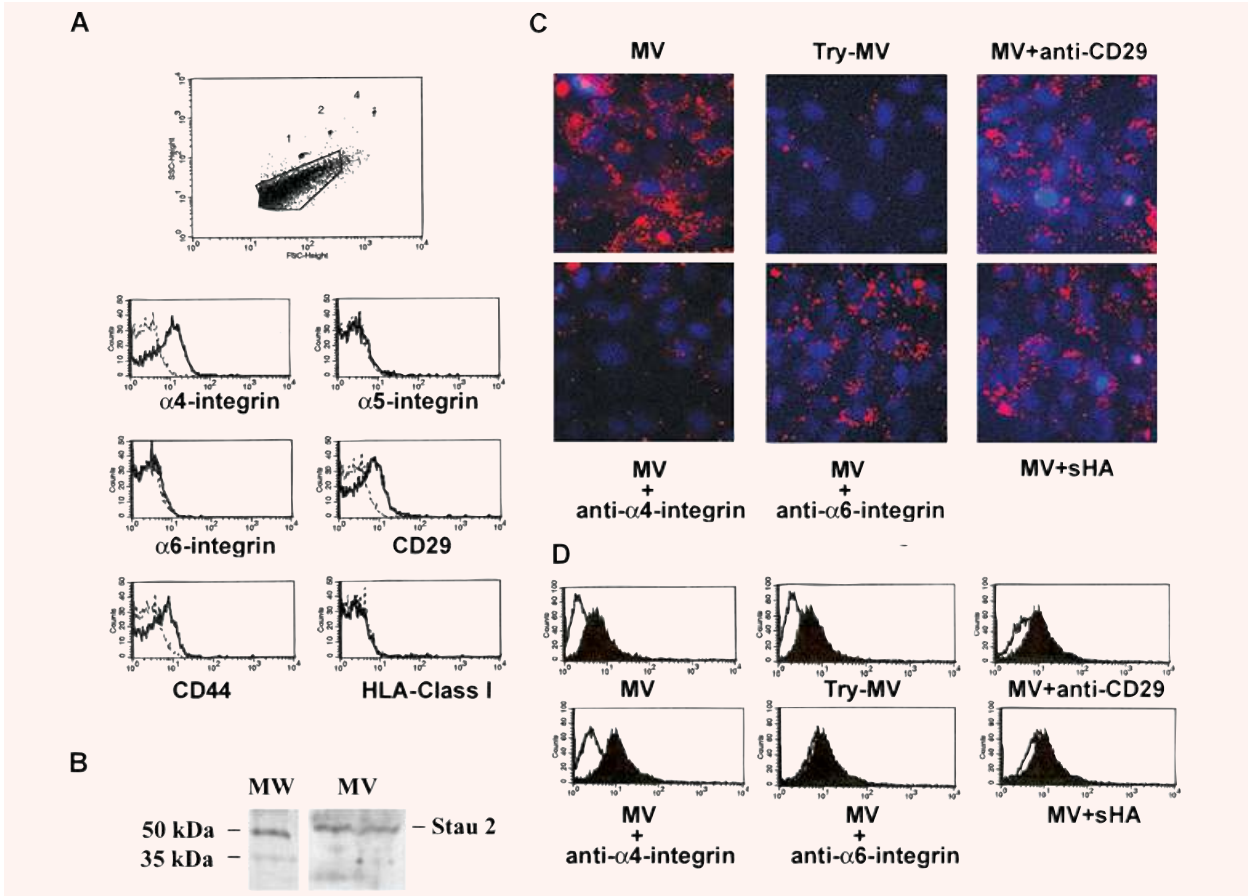

Fig. 1 Cytofluorimetric characterization of HLSC-derived MVs and their incorporation into hepatocytes. (**A**) Representative FACS analyses of MVs showing the size (with 1-, 2- and 4-μm beads used as internal size standards) and the expression of α_4-integrin, α_5-integrin, α_6-integrin, CD29, CD44 and HLA-class I (dark lines) surface molecules. Dot lines indicate the isotypic controls. Ten different MV preparations were analysed with similar results. In the α_4-integrin, CD29, CD44 experiments the Kolmogrov–Smirnov statistical analyses between relevant antibodies and the isotypic control was significant ($P < 0.001$). No significant expression of α_5-integrin, α_6-integrin and HLA class I was observed. (**B**) Western blot analysis of two different MV preparations showing the expression of Staufen 2 (Stau 2) ribonucleoprotein. (**C**) Representative confocal microscopy micrographs of internalization by human hepatocytes (3 hrs at 37°C) of MVs labelled with red fluorescent PKH26. Where indicated MVs were pre-incubated trypsin (0.5 mM; Try-MV), with 1 μg/ml blocking monoclonal antibodies against CD29, α_4- and α_6-integrin or with 100 μg/ml of sHA to block CD44. Three experiments were performed with similar results. Original magnification: ×630. (**D**) Representative FACS analyses of internalization by hepatocytes of MVs labelled with PKH26 (black areas) pre-incubated with trypsin (0.5 mM; Try-MV) or with 1 μg/ml blocking monoclonal antibodies against CD29, α_4- and α_6-integrin or sHA. Black areas indicate the internalization of untreated MVs. In the first panel white area indicates the negative control (cells incubated with vehicle alone). In the other panels white areas indicate internalization of MVs after incubation trypsin or with blocking antibodies or sHA. Three experiments were performed with similar results.

Calco, Italy) weighing 180–200 g were anesthetized and subjected to 70% hepatectomy as previously described [17]. In sham-operated animals, livers were briefly exposed outside the peritoneal cavity. Immediately after hepatectomy, animals received an intravenous injection of 30 μg HLSC-derived MVs either untreated or RNase treated. Control rats received an equal volume of saline i.p. To measure hepatocyte proliferation in excised livers, rats received an i.p. injection of BrdU (100 mg/kg) 2 hrs before being killed as suggested by Lanier *et al.* [32] for the evaluation of hepatocellular proliferation in rodents. Rats were killed at 8, 24, 48 or 72 hrs after surgery to collect the remnant liver. Blood was also withdrawn from the abdominal aorta and serum was obtained by centrifugation (3000 rpm, 20 min.) to measure alanine transaminase (ALT), aspartate transaminase (AST) and albumin. Six animals were used for each time point. Liver samples were snap frozen in liquid nitrogen and stored at −80°C until used in molecular biology studies. Additional liver samples were paraffin embedded for histology, immunohistochemistry and immunofluorescence analysis. Body and liver weights were recorded at each post-operative time to assess liver regeneration rate that was expressed as the ratio wet liver weight to body weight (%) [33].

Table 1 MV-shuttled mRNA involved in transcription, translation and cell proliferation

Functional category	mRNA	Description
Transcription regulators	CASP8AP2	CASP8 associated protein 2
	DMRT2	Doublesex and mab-3 related transcription factor 2
	HOXC12	Homeobox C12
	NFIX	Nuclear factor I/X (CCAAT-binding transcription factor)
	HOXA3	Homeobox C3
	MIB2	Mindbomb homolog 2
	NFIX	Nuclear factor I/X
	NR2E3	Nuclear receptor subfamily 2
	SIM2	Single-minded homolog 2
Translation regulator	EIF2C2 (AGO2)	Eukaryotic translation initiation factor 2C, 2
Enzymes/metabolism	CREG2	Cellular repressor of E1A-stimulated genes 2
	FKBP9	FK506 binding protein 9, 63 kD
	IMPDH1	IMP (inosine monophosphate) dehydrogenase 1
	MRE11A	MRE11 meiotic recombination 11 homolog A (S. cerevisiae)
	ST3GAL4	ST3 β-galactoside α-2,3-sialyltransferase 4
	STK40	Serine/threonine kinase 40
	ACPP	Acid phosphatase, prostate
	PGC	Progastricsin (pepsinogen C)
	B3GAT1	β-1,3-glucuronyl-transferase 1
	CDK2	Cyclin-dependent kinase 2
	CHEK2	Cell cycle checkpoint regulator
	LTK	Leucocyte receptor tyrosine kinase
	MATK	Megakaryocyte-associated tyrosine kinase
	PTEN	Phosphatase and tensin homolog
	PTPN2	Protein tyrosine phosphatase
Transporter	AP3M2	Adaptor-related protein complex 3, mu 2 subunit
	ATP1A2	ATPase, Na^+/K^+ transporting, α_2^+ polypeptide
	PODXL	ATP binding
	SLC22A16	Organic cation/carnitine transporter
Ion channel	CACNG1	Calcium channel, voltage-dependent, γ subunit 1
G-protein coupled receptor	MC3R	Melanocortin 3 receptor
Other	TMEM179	Transmembrane protein 179
	TOR1AIP2	Torsin A interacting protein 2
	TSPAN7	Tetraspanin 7
	VASP	Vasodilator-stimulated phosphoprotein

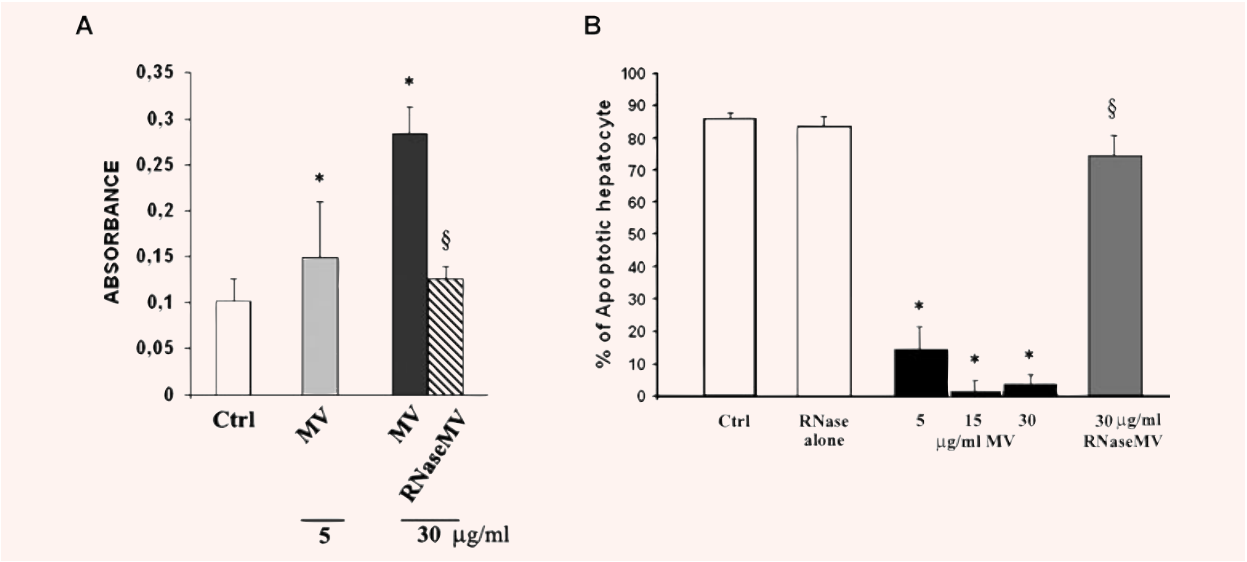

Fig. 2 Proliferative and anti-apoptotic effects of HLSC-derived MVs on human hepatocytes. (**A**) 10 μM BrdU was added to 50,000 cells/well into 48-well plates incubated for 48 hrs in William's E medium deprived of FCS in the presence of vehicle alone (Ctrl; white bar) or of MVs (5 μg/ml grey bar; 30 μg/ml dark bar) or of RNase-treated MVs (shaded bar). Results are expressed as mean ± S.D. of three different experiments performed in triplicate. Analyses of variance with Newmann–Keuls multicomparison test was performed; $*P < 0.05$ MV *versus* vehicle alone (Ctrl); §$P < 0.05$ MV treated with RNase *versus* MV untreated. (**B**) The percentage of apoptotic cells was evaluated by the TUNEL assay. We used, as apoptotic stimulus, HLSC incubated with 5 mM GalN for 24 hrs in DMEM supplemented with 2% FCS. Controls (white bars) included hepatocytes incubated with vehicle alone (Ctrl) and hepatocytes incubated with vehicle containing RNase submitted to the same procedure of inactivation as in samples of RNase-treated MVs as described in 'Material and methods' (RNase alone); hepatocytes incubated with 5, 15, 30 μg/ml MVs (black bars); hepatocytes incubated with RNase-treated MVs (grey bar). Results are expressed as mean ± S.D. of three different experiments performed in duplicate. Analyses of variance with Newmann–Keuls multicomparison test was performed; $*P < 0.05$ MV *versus* vehicle alone; §$P < 0.05$ MV RNase treated *versus* MV untreated.

Morphological studies

For hepatic histology, 5-μm-thick paraffin liver sections were routinely stained with haematoxylin and eosin. Immunohistochemistry for detection of hepatocyte proliferation was performed as previously described [34] using anti-BrdU (Dakocytomation) or anti-PCNA (Santa Cruz Biotechnology, Santa Cruz CA, USA) monoclonal antibodies. Ten non-consecutive sections were counted for $BrdU^+$ and $PCNA^+$ hepatocytes at 200× magnification. Confocal microscopy analysis was performed on frozen sections for detection of specific human AGO2 protein. Sections were blocked and labelled with rabbit anti-human AGO2 (Abcam) (1:300 dilution). Omission of the primary antibodies or substitution with non-immune rabbit IgG was used as controls. Alexa Fluor 488 anti-rabbit (Molecular Probes) was used as secondary antibody. Hoechst 33258 dye (Sigma) was added for nuclear staining.

Oil red O staining for hepatic triglyceride detection

Frozen liver sections were assayed by a modification of the Folch method for triglyceride content using Oil red O staining [34]. Frozen sections of liver were fixed for 10 min. in neutral buffered 10% formalin and stained with Oil red O (Sigma) for 10 min., counterstained with haematoxylin for 2 min., and cover slipped with a water-based mounting medium.

Biochemical analyses

Serum ALT and AST levels were measured using a standard clinical automatic analyser. Serum rat albumin was determined by ELISA (Alpco diagnostic, Salem, NH, USA).

Statistical analysis

Data were analysed using the t-tests, ANOVA with Newmann–Keuls' or ANOVA with Dunnet's multicomparison tests as appropriate. A *P*-value of <0.05 was considered significant.

Results

Characterization of HLSC-derived MVs

By cytofluorimetric analyses MVs produced by HLSC were detected mainly below the forward scatter signal corresponding to 1-μm beads (Fig. 1A). When determined by Zetasizer, the size of MVs

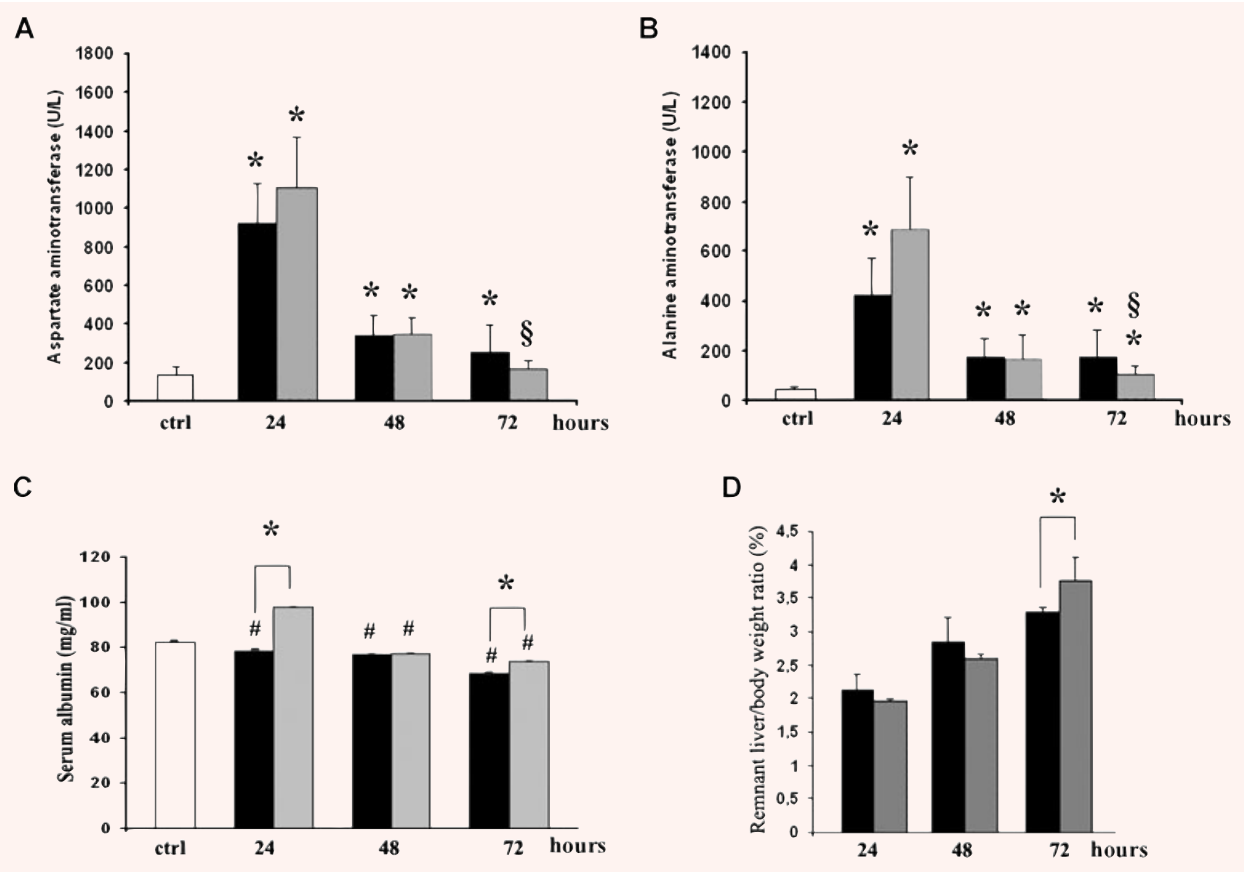

Fig. 3 Effect of MVs on biochemical parameters and on remnant liver/body weight ratio into 70% herpatectomized rats. (**A**) Aspartate aminotransferase, (**B**) alanine aminotransferase were measured in serum in sham operated rats (Ctrl; white bars), in 70% hepatectomized rats (black bars) and in 70% hepatectomized rats treated with 30 μg/ml MVs (grey bars) and expressed as U/L. Data are expressed as mean ± S.D. relative quantity of six different rats per group. Analyses of variance with Newmann–Keuls multicomparison test was performed; $*P < 0.05$ MV *versus* Ctrl; §$P < 0.05$ MV treated rats *versus* MV untreated. (**C**) Albumin was measured in serum of sham operated rats (Ctrl; white bar), in 70% hepatectomized rats (black bars) and in 70% hepatectomized rats treated with 30 μg/ml MVs (grey bars) and expressed as mg/ml. Data are expressed as mean ± S.D. relative quantity of six different rats per group. Analyses of variance with Newmann–Keuls multicomparison test was performed; $*P < 0.05$ MV treated rats *versus* MV untreated; $\#P < 0.05$ all experimental groups *versus* Ctrl. (**D**) Remnant liver/body weight ratio was evaluated into 70% hepatectomized rats MV untreated (black bars) or MV treated (gray bars). Data are expressed as mean 6 S.D. relative quantity of six different rats per group. T student test $*P < 0.05$ treated rats *versus* MV untreated.

ranged from 80 nm to 1 μm, with a mean value of 195 nm. Cytofluorimetric analyses showed the presence of several adhesion molecules also present on HLSC plasma membrane such as α_4-integrin, CD29 and CD44. MVs did not express α_5- and α_6-integrins and HLA-class I (Fig. 1A) at variance with the cells of origin [18].

Gene array analyses of HLSC-derived MVs

mRNA extracted from MVs was submitted to microarray analysis to define which transcripts were present [21]. A total of 65 transcripts were found with this procedure; 60 were associated to Entrez gene identifiers [30] by IPA 6.0 analysis (see additional information). This observation indicated that MVs shuttled a specific subset rather than a random sample of cellular mRNA. MVs contained mRNA related to several cell functions involved in the control of transcription and metabolism (Table 1). In particular the following genes, that were detected in MVs, are known to be involved in cell proliferation: MATK, MRE11A, CHECK2, MYH11, VASP and CDK2. In particular, CDK2 gene has been shown to be involved in liver regeneration [35]. Moreover, MVs contained the AGO2 (EIF2C2) gene which is a translation

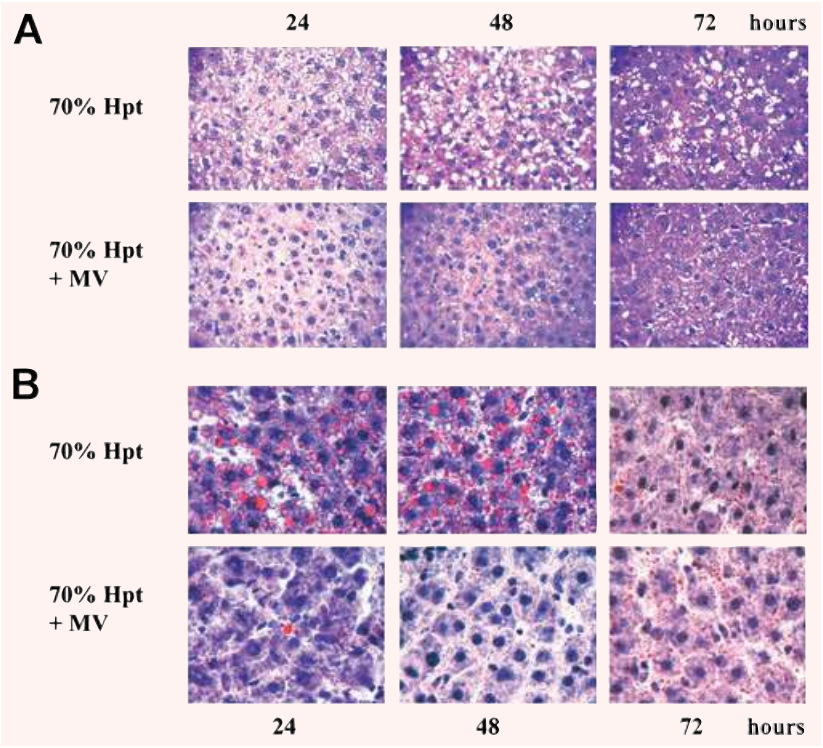

Fig. 4 Effects of MVs on histological changes into 70% hepatectomized rats. Representative light microscopy micrographs of liver histology at 24, 48 and 72 hrs after 70% hepatectomy (70% Hpt) in rats injected or not with 30 μg of MVs. (**A**) Haematoxylin & Eosin staining; (**B**) Oil red O staining for triglycerides. Original magnification: ×200.

regulator with a critical role in the control of microRNA production [36]. Quantitative real time PCR confirmed the presence in MVs of genes randomly chosen from those detected by Microarray *(AGO2*, *CHEK2*, *CDK2*, *MATK*).

Moreover, MVs were shown to contain Staufen 2 (Fig. 1B) a ribonucleoprotein involved in the transport and stability of mRNA [37].

Incorporation of MVs in cultured hepatocytes

MVs labelled with PKH26 dye were incorporated by cultured human hepatocytes after 3 hrs of incubation at 37°C as shown by FACS analysis and confocal microscopy (Fig. 1A, C). In order to investigate the role of adhesion molecules expressed by the MV surface in the incorporation in target cells, MVs were pre-incubated (15 min., at 4°C) with blocking antibodies against the identified adhesion molecules or with sHA to block CD44 (Fig. 1C, D). MV treatment with anti-α_4-integrin blocking antibody inhibited MV incorporation in human hepatocytes. Blockade of CD44 or CD29 only slightly reduced incorporation of MVs (Fig. 1D). The anti-α_6-integrin blocking antibody used as negative control did not prevent MV internalization. Moreover, removal of surface molecules by trypsin treatment of MVs inhibited their incorporation in human hepatocytes confirming the relevance of surface expressed molecules in the process of MV internalization by target cells. Similar results were obtained using rat hepatocytes (data not shown).

In vitro proliferative and anti-apoptotic effects of MVs

Incubation of human hepatocytes with MVs derived from HLSC promoted a significant proliferation in respect to control cells incubated with vehicle alone (Fig. 2A). In addition, incubation of human hepatocytes with increasing doses of MVs significantly inhibited apoptosis induced by GalN (Fig. 2B). However, when MVs were incubated with RNase, that we previously showed to induce a complete degradation of the RNA shuttled by MVs without affecting their structure [23], proliferation and apoptosis resistance elicited by MVs were significantly reduced (Fig. 2A, B). As previously shown [23], RNase treatment did not modify the expression of surface molecules or the internalization of MVs (not shown). These results suggest that the MV biological effects were mediated by the transfer of mRNA following MV internalization, as previously described [21, 23]. DNase treatment was ineffective (not shown).

HLSC-derived MVs enhanced hepatic regeneration in rat with 70% hepatectomy

In the rat model of 70% hepatectomy, we observed a significant rise in AST and ALT and a significant reduction in serum albumin at 24, 48 and 72 hrs (Fig. 3A–C). In MV-treated rats the rise of AST

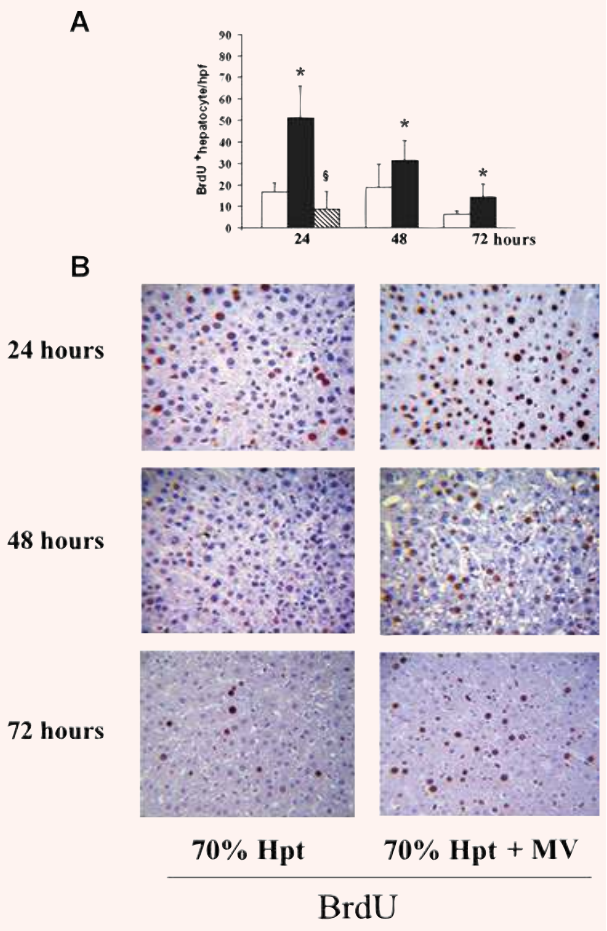

Fig. 5 Effect of MVs on liver cell proliferation evaluated as BrdU incorporation in 70% hepatectomized rats. (**A**) Quantification of $BrdU^+$ cells/high power field (hpf). BrdU was injected intraperitoneally 2 hrs before rats being killed. Hepatectomized rats injected with vehicle = white bars; hepatectomized rats injected with 30 μg MVs = black bars; hepatectomized rats injected with 30 μg RNase-treated MVs = shaded bars. Data are expressed as mean ± S.D. relative quantity of six different rats per group. Analyses of variance with Newmann–Keuls multicomparison test was performed; $*P < 0.05$ MV treated *versus* MV untreated rats; §$P < 0.05$ rats injected with RNase-treated MVs *versus* rats injected with MVs. (**B**) Representative micrographs of BrdU uptake performed on sections of livers 24, 48 and 72 hrs after 70% hepatectomy in rats treated with vehicle (70% Hpt) or treated with 30 μg MVs (70% Hpt + MV). Original magnification: ×200.

and ALT was significantly lower after 72 hrs (Fig. 3A, B) in respect to the untreated. Moreover, in MV-treated rats an enhanced production of albumin was detected at 24 hrs (Fig. 3C). The liver/body weight ratio gradually increased after 70% hepatectomy in rats treated or not with MVs. However, after 72 hrs a significant enhancement of liver/body ratio was observed in MV-treated in respect to untreated rats (Fig. 3D). The histological examination of 70% hepatectomized rats showed a marked hepatocyte swelling and vacuolization (Fig. 4A). The staining for triglyceride with Oil red O indicated a diffuse hepatic steatosis (Fig. 4B). When animals were treated with MVs, the lesions were less severe at all the time points in respect to animals with 70% hepatectomy treated with vehicle alone (Fig. 4A) and the steatosis was minimal or absent (Fig. 4B). As shown in Figs 5 and 6, MV-treatment of rats with 70% hepatectomy significantly enhanced *in vivo* hepatocyte proliferation as detected by $BrdU^+$ and $PCNA^+$ cells in respect to hepatectomized rats injected with vehicle alone (Figs 5A, B and 6A, B). The enhanced proliferation was detected at all the different time points after MV treatment. RNase treatment of MVs abrogated MV-induced recovery of liver lesions and significantly inhibited hepatic proliferation induced by MVs (Figs 5A and 6A). The activation of a proliferative program in hepatocytes was also confirmed by Q-PCR showing a significantly enhanced expression of cyclin A1 in rats treated with MVs in respect to the untreated (Fig. 6C).

After hepatectomy a significant enhancement of apoptosis of hepatocytes was seen only after 72 hrs (Fig. 7A, B). When hepatectomized rats were treated with MVs, a significant reduction of apoptosis was observed.

In vivo evidence of *de novo* human protein expression in the liver of hepatectomized rats treated with human MVs

Q-PCR and RT-PCR for human AGO2, used as reporter gene, confirmed the accumulation of injected MVs within the liver of hepatectomized rats treated with MVs but not in those treated with vehicle alone (Fig. 8A, B). Using anti-human AGO2 antibody, the protein was detected both by Western blot analysis (Fig. 8C) of liver extracts and by immunofluorescence (Fig. 8D) in hepatectomized rats treated with MVs but not in those treated with vehicle alone. By confocal microscopy AGO2 protein was detected with a perinuclear localization in liver parenchyma. HLSC-derived MVs contained AGO2 mRNA (Table 1) but not the protein (not shown). These observations suggest that human specific mRNA shuttled by MVs could be translated in protein in liver cells during regeneration.

Discussion

In the present study, we demonstrated that MVs derived from human HLSC promoted hepatocyte proliferation and suppressed hepatocyte cell death. MV administration accelerated *in vivo* liver regeneration in 70% hepatectomized rats. The RNase treatment of MVs abrogated both the *in vitro* and *in vivo* effects of MVs, suggesting that the RNA shuttled by MVs was the final effector of their biological effect.

The 70% hepatectomy in rats is a classical model to study liver regeneration. The remaining hepatic lobes of the rats can restore

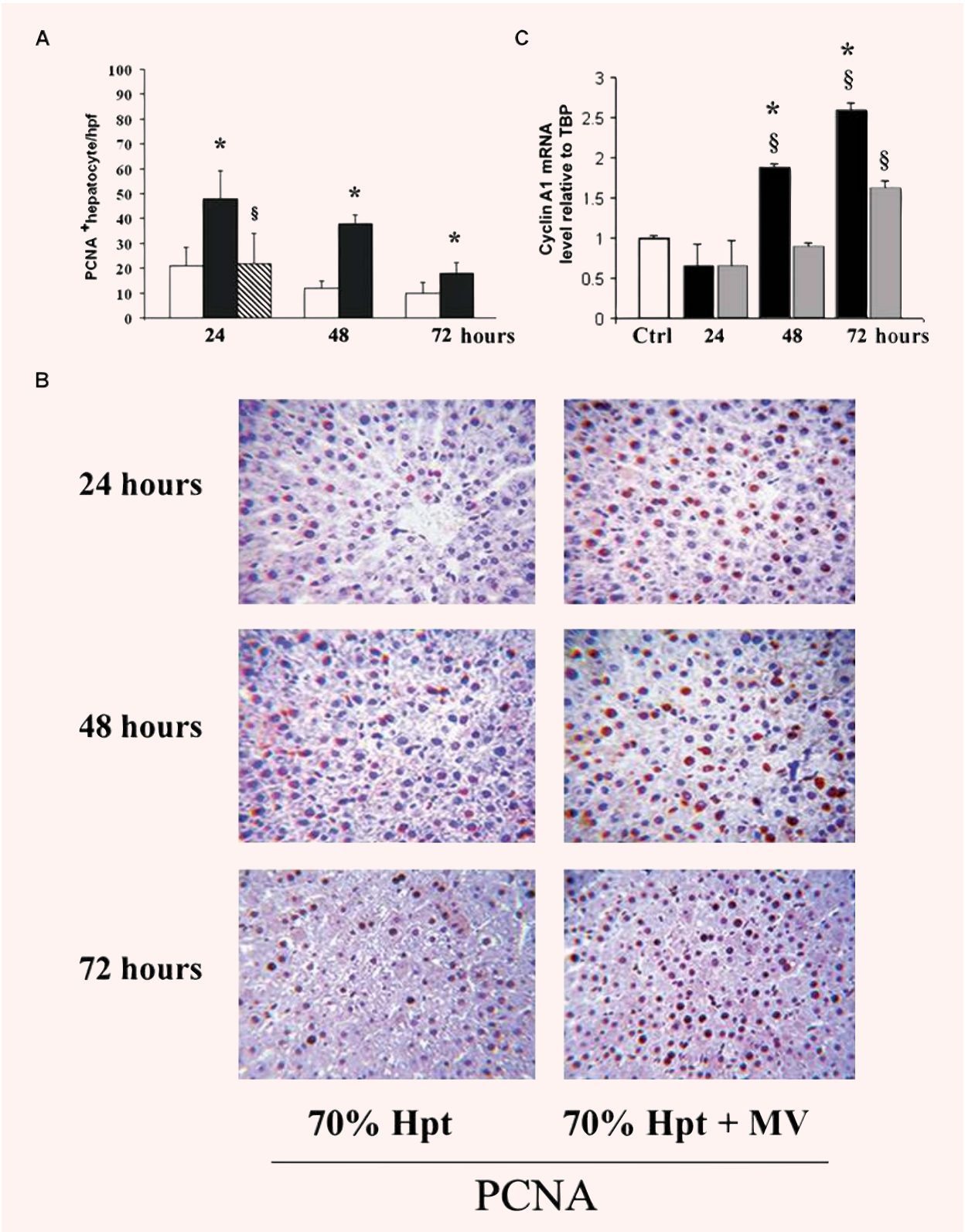

Fig. 6 Effect of MVs on liver cell proliferation evaluated as PCNA and Cyclin A1 expression in 70% hepatectomized rats. (**A**) Quantification of PCNA$^+$ cells/hpf. Hepatectomized rats injected with vehicle 5 white bars; hepatectomized rats injected with 30 μg MVs = black bars; hepatectomized rats injected with 30 μg RNase-treated MVs = shaded bars. Data are expressed as mean ± S.D. relative quantity of six different rats per group. Analyses of variance with Newmann–Keuls multicomparison test was performed; *$P < 0.05$ MV treated *versus* MV untreated rats; §$P < 0.05$ rats injected with RNase-treated MVs *versus* rats injected with MVs. (**B**) Representative micrographs of PCNA staining performed on sections of livers 24, 48 and 72 hrs after 70% hepatectomy in rats treated with vehicle (70% Hpt) or treated with 30 μg MVs (70% Hpt + MV). Original magnification: ×200. (**C**) Real time PCR for cyclin A1 (CCNA1) on tissue extract of normal liver (Ctrl; white bars) or liver of hepatectomized rats treated with 30 μg MVs (black bars) or of sham operated rats injected with vehicle alone(grey bar). Data are expressed as mean ± S.D. relative quantity of six different rats per group. Analyses of variance with Newmann–Keuls multicomparison test was performed; *$P < 0.05$ *versus* MV treated rats *versus* untreated; §$P < 0.05$ all groups *versus* shame operated rats.

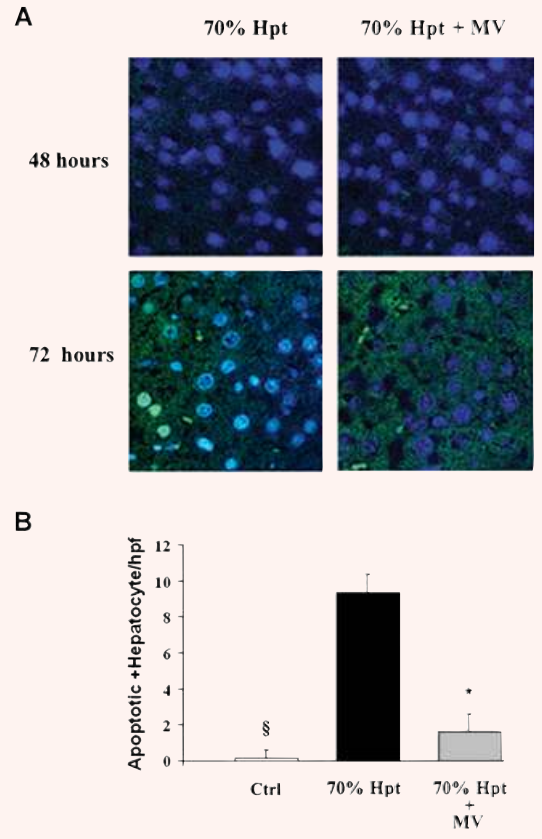

Fig. 7 Effect of MVs on apoptosis in 70% hepatectomized rats. (**A**) Representative micrographs of TUNEL on liver sections of 70% hepatectomized rats injected with vehicle (70% Hpt) or injected with 30 μg MVs (70% Hpt + MV) and killed at 48 and 72 hrs (6 rats per group). Original magnification ×630. (**B**) Quantification of TUNEL$^+$ cells/hpf at 72 hrs in shame operated rats (Ctrl; white bar) or after hepatectomy in rats injected with vehicle (black bar) and in rats injected with 30 μg MVs (grey bar). Data are expressed as mean ± S.D. relative quantity of six different rats per group. Analyses of variance with Newmann–Keuls multicomparison test was performed; *$P < 0.05$ hepatectomized rats *versus* sham operated rats; §$P < 0.05$ rats injected with MVs *versus* rats injected with vehicle alone.

the liver mass two weeks after partial hepatectomy [17]. It has been suggested that the regeneration process is due to the proliferation of residual mature hepatocytes that re-enter into the cell cycle and undergo proliferation [8]. It is not clear whether resident or bone marrow derived stem cells may contribute to liver regeneration and whether resident stem cells may orchestrate the cell cycle entry of differentiated cells [9]. Recently, Quesenberry and Aliotta [19] proposed a dynamic reconsideration of the stem cell niches suggesting that the lability of stem cell phenotype depends on complex interactions with differentiated cells based on MV mediated cell-to-cell transfer of genetic information. Moreover, these authors suggested that transfer of genetic information from injured cells may explain stem cell functional and phenotypic changes without the need of transdifferentiation into tissue cells [19]. On the other hand, we showed that transfer of genetic information from stem cells may re-direct altered functions in target cells suggesting that stem cells may repair damaged tissues without directly replacing parenchymal cells [21, 23]. Indeed, the genetic information shuttled by MVs may be exploited to activate angiogenic and regenerative programs in target cells [21, 23].

Shedding of MVs is no longer considered an artefact [38, 39] and it has been shown to occur *in vivo* [24]. It has been suggested that shedding vesicles could participate in important biological processes and their significant number at the surface of a Cajal-like cell of the heart [24] suggests that these structures may transport important information to other cells.

In the present study, we demonstrated that MVs derived from HLSC may induce *in vitro* proliferation and apoptosis resistance in human and rat hepatocytes. HLSC is a pluripotent stem cells population resident in the adult human liver [18]. *In vivo* HLSC were shown to contribute to liver regeneration in a model of acute liver injury in SCID mice [18]. In the present study we found that HLSC spontaneously released MVs in culture. MVs released from HLSC had a size similar to that described for MVs released from endothelial progenitors cells [21] or from bone marrow derived mesenchymal stem cells [23] and expressed several adhesion molecules known to be present on the surface of HLSC such as CD44, CD29 (b1-integrin), α_4-integrin. It has been previously reported that the adhesion molecules expressed by MVs are instrumental in their internalization into target cells [40]. We found that α_4-integrin blockade prevented MV incorporation into hepatocytes whereas blockade of CD44 and CD29 had only minor effects.

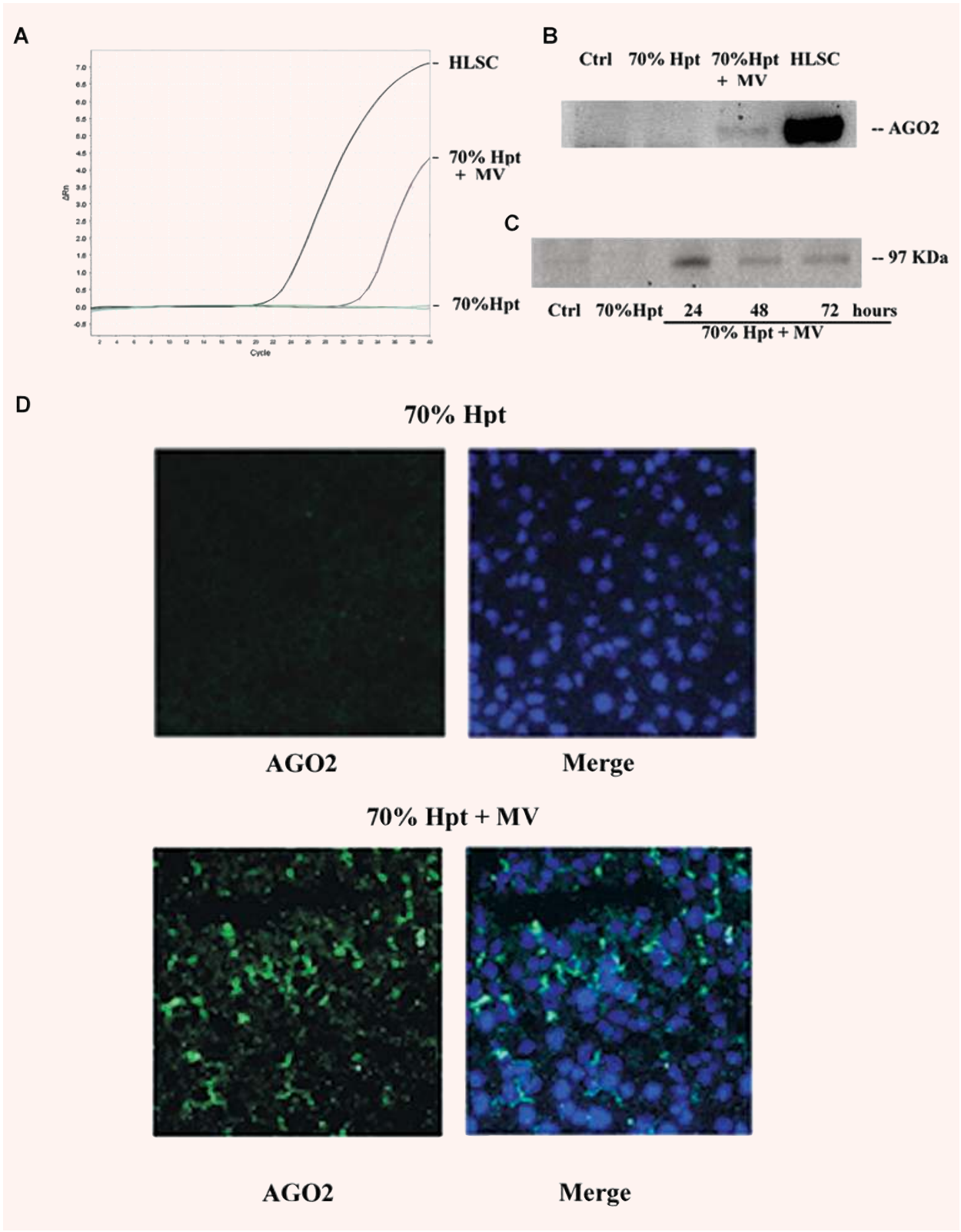

Fig. 8 Detection of human mRNA and human protein expression in livers of rats treated with MVs. (**A**) Representative amplification plot of Q-PCR for human AGO2 of liver extracts of hepatectomized rats untreated (70% Hpt) or treated with 30 μg MVs (70% Hpt + MV) and killed 8 hrs after hepatectomy. HLSC were used as positive control. (**B**) Representative RT- PCR for human AGO2 on liver extracts of hepatectomized rats untreated (70% Hpt) or treated with 30 μg MVs (70% Hpt + MV) and killed 8 hrs after hepatectomy. HLSC were used as positive control and liver from shamed operated rats as negative control (Ctrl). A band of the expected size (100 pb) were detected in a 4% Agarose gel electrophoresis. (**C**) Representative immunoprecipitation for human AGO2 of liver extracts of hepatectomized rats untreated (70% Hpt) killed 24 hrs after hepatectomy or of rats treated with 30 μg MVs (70% Hpt + MV) killed 24, 48 or 72 hrs after hepatectomy. (**A**), (**B**) and (**C**) Three experiments were done with similar results. (**D**) Representative confocal micrographs showing the perinuclear expression of human AGO2 protein in liver sections of 70% hepatectomized rats treated or not with MVs and killed 72 hrs later. Nuclei were counterstained with Hoechst dye. Original magnification: ×630. Six rats per group were studied with similar results.

The internalization of MVs in target cells was previously found to be essential for their biologic activity but not the final mechanism of action [40]. Indeed, RNase treatment almost completely abrogated MV-induced angiogenic and regenerative effects suggesting a critical role of RNA transfer mediated by MVs [21, 23]. In the present study, we found that MV treatment with RNase abrogated the *in vitro* proliferation and resistance to apoptosis of hepatocytes.

The *in vivo* administration of MVs derived from HLSC was found to accelerate liver regeneration in 70% hepatectomized rats. This was possibly related to an *in vivo* stimulation of proliferation of hepatocytes, as indicated by the incorporation of BrdU, the expression of PCNA and of cyclin A1 by hepatocytes. Moreover, MV treatment significantly reduced liver apoptosis as seen by TUNEL. Pre-treatment of MVs with RNase abrogated also the protective effect of MVs in 70% hepatectomized rats. One can speculate that the delivery of exogenous mRNA by MVs to hepatocytes may stimulate hepatic regeneration. Indeed, MVs derived from HLSC contained a defined pattern of mRNA associated with several cell functions involved in the control of transcription, translation and proliferation. *In vivo* evidence for an effective horizontal transfer of mRNA was obtained by the presence of the human specific mRNA for AGO2, chosen as reporter gene, and by its *de novo* protein expression in the liver of MV-treated hepatectomized rats. AGO2 is a regulatory protein with a central role in RNA silencing processes [36]. The results of present study are in line with the recent evidence that MVs may shuttle biologically active mRNA or microRNA able to regulate cell function of different target cells [20–23, 41–43]. Of interest, the pattern of genes present in HLSC-derived MVs was substantially different from that of endothelial precursors and mesenchymal stem cells [21, 23] indicating a specificity for the cell of origin. Moreover, MVs were shown to contain Staufen 2 suggesting a role of ribonucleoproteins in carrying and stabilizing RNAs [37] within MVs.

In conclusion, MV-mediated transfer of mRNA from HLSC to hepatocytes may represent a mechanism that contribute to liver regeneration and that could be exploited in regenerative medicine.

Acknowledgements

This work was supported by Fresenius Medical Care and by Regione Piemonte, progetto PISTEM.

Supporting Information

Additional Supporting Information may be found in the online version of this article:

Table S1 MV associated transcript linked to Egs by IPA 5.0 (www.ingenuity.com)

Please note: Wiley-Blackwell are not responsible for the content or functionality of any supporting materials supplied by the authors. Any queries (other than missing material) should be directed to the corresponding author for the article.

References

1. **Fiegel HC, Lange C, Kneser U *et al.*** Fetal and adult liver stem cells for liver regeneration and tissue engineering. *J Cell Mol Med.* 2006; 10: 577–87.
2. **Alison MR, Choong C, Lim S.** Application of liver stem cells for cell therapy. *Semin Cell Dev Biol.* 2007; 18: 819–26.
3. **Seo MJ, Suh SY, Bae YC *et al.*** Differentiation of human adipose stromal cells into hepatic lineage *in vitro* and *in vivo*. *Biochem Biophys Res Commun.* 2005; 328: 258–64.
4. **Lagasse E, Connors H, Al-Dhalimy M *et al.*** Purified hematopoietic stem cells can differentiate into hepatocytes *in vivo*. *Nat Med.* 2000; 6: 1229–34.
5. **Sato Y, Araki H, Kato J *et al.*** Human mesenchymal stem cells xenografted directly to rat liver are differentiated into human hepatocytes without fusion. *Blood.* 2005; 106: 756–63.
6. **Aurich I, Mueller LP, Aurich H *et al.*** Functional integration of hepatocytes derived from human mesenchymal stem cells into mouse livers. *Gut.* 2007; 56: 405–15.
7. **Cai J, Zhao Y, Liu Y *et al.*** Directed differentiation of human embryonic stem cells

into functional hepatic cells. *Hepatology*. 2007; 45: 1229–39.
8. **Michalopoulos GK.** Liver regeneration. *J Cell Physiol*. 2007; 213: 286–300.
9. **Alison MR, Poulsom R, Jeffery R *et al.*** Hepatocytes from non-hepatic adult stem cells. *Nature*. 2000; 406: 257.
10. **Petersen BE, Bowen WC, Patrene KD *et al.*** Bone marrow as a potential source of hepatic oval cells. *Science*. 1999; 284: 1168–17.
11. **Miyashita H, Suzuki A, Fukao K *et al.*** Evidence for hepatocyte differentiation from embryonic stem cells *in vitro*. *Cell Transplant*. 2002; 11: 429–34.
12. **Parekkadan B, van Poll D, Suganuma K *et al.*** Mesenchymal stem cell-derived molecules reverse fulminant hepatic failure. *Plos One*. 2007; 2: e941.
13. **Van Poll D, Parekkadan B, Cho CH *et al.*** Mesenchymal stem cell-derived molecules directly modulate hepatocellular death and regeneration *in vitro* and *in vivo*. *Hepatology*. 2008; 47: 1634–43.
14. **Leedham SJ, Brittan M, McDonald SA *et al.*** Intestinal stem cells. *J Cell Mol Med*. 2005; 9: 11–24.
15. **Cantley LG.** Adult stem cells in the repair of the injured renal tubule. *Nat Clin Pract Nephrol*. 2005; 1: 22–32.
16. **Mandache E, Vidulescu C, Gherghiceanu M *et al.*** Neoductular progenitor cells regenerate hepatocytes in severely damaged liver: a comparative ultrastructural study. *J Cell Mol Med*. 2002; 6: 59–73.
17. **Higgins GH, Anderson RM.** Experimental pathology of the liver. Restoration of the liver in the white rat following partial surgical removal. *Arch Pathol*. 1931; 12: 186–202.
18. **Herrera MB, Bruno S, Buttiglieri S *et al.*** Isolation and characterization of a stem cell population from adult human liver. *Stem Cells*. 2006; 24: 2840–50.
19. **Quesenberry PJ, Aliotta JM.** The paradoxical dynamism of marrow stem cells: considerations of stem cells, niches, and microvesicles. *Stem Cell Rev*. 2008; 4: 137–47.
20. **Ratajczak J, Miekus K, Kucia M *et al.*** Embryonic stem cell-derived microvesicles reprogram hematopoietic progenitors: evidence for horizontal transfer of mRNA and protein delivery. *Leucemia*. 2006; 20: 847–56.
21. **Deregibus MC, Cantaluppi V, Calogero R *et al.*** Endothelial progenitor cell derived microvesicles activate an angiogenic program in endothelial cells by a horizontal transfer of mRNA. *Blood*. 2007; 110: 2440–8.
22. **Ratajczak J, Wysoczynski M, Hayek F *et al.*** Membrane-derived microvesicles: important and underappreciated mediators of cell-to-cell communication. *Leucemia*. 2006; 20: 1487–95.
23. **Bruno S, Grange C, Deregibus MC *et al.*** Human mesenchymal stem cell-derived microvesicles protect against acute tubular injury. *J Am Soc Nephrol*. 2009; 20: 1053–67.
24. **Kostin S, Popescu LM.** A distinct type of cell in myocardium: interstitial Cajal-like cells. *J Cell Mol Med*. 2009; 13: 295–308.
25. **Hinescu ME, Popescu LM.** Interstitial Cajal-like cells (ICLC) in human atrial myocardium. *J Cell Mol Med*. 2005; 9: 972–5.
26. **Dunn JC, Yarmush ML, Koebe HG *et al.*** Hepatocyte function and extracellular matrix geometry: long-term culture in a sandwich configuration. *FASEB J*. 1989; 3: 174–7.
27. **Bussolati B, Deambrosis I, Russo S *et al.*** Altered angiogenesis and survival in human tumor-derived endothelial cells. *FASEB J*. 2003; 17: 1159–61.
28. **Siendones E, Fouad D, Abou-Elella AMKE *et al.*** Role of nitric oxide in D-galactosamine-induced cell death and its protection by PGE1 in cultured hepatocytes. *Nitric Oxide*. 2003; 8: 133–43.
29. **Gentleman RC, Carey VJ, Bates DM *et al.*** Bioconductor: open software development for computational biology and bioinformatics. *Genome Biol*. 2004; 5: R80.
30. **Bolstad BM, Irizarry RA, Astrand M *et al.*** A comparison of normalization methods for high density oligonucleotide array data based on variance and bias. *Bioinformatics*. 2003; 19: 185–93.
31. **Collino F, Bussolati B, Gerbaudo E *et al.*** Preeclamptic sera induce nephrin shedding from podocytes through endothelin-1 release by endothelial glomerular cells. *Am J Physiol Renal Physiol*. 2008; 294: 1185–94.
32. **Lanier TL, Berger EK, Eacho PI.** Comparison of 5-bromo-2-deoxyuridine and [3H]thymidine for studies of hepatocellular proliferation in rodents. *Carcinogenesis*. 1989; 10: 1341–3.
33. **Hamada T, Eguchi S, Yanaga K *et al.*** The effect of denervation on liver regeneration in partially hepatectomized rats. *J Surg Res*. 2007; 142: 170–4.
34. **Shteyer E, Liao Y, Muglia LJ *et al.*** Disruption of hepatic adipogenesis is associated with impaired liver regeneration in mice. *Hepatology*. 2004; 40: 1322–32.
35. **Stärkel P, De Saeger C, Sempoux C *et al.*** Blunted DNA synthesis and delayed S-phase entry following inhibition of Cdk2 activity in the regenerating rat liver. *Lab Invest*. 2005; 85: 562–71.
36. **Lingel A, Isaurralde E.** RNAi: finding the elusive endonuclease. *RNA*. 2004; 10: 1675–9.
37. **Miki T, Takano K, Yoneda Y.** The role of mammalian Staufen on mRNA traffic: a view from its nucleocytoplasmic shuttling function. *Cell Struct Funct*. 2005; 30: 51–6.
38. **Lakkaraju A, Rodriguez-Boulan E.** Itinerant exosomes: emerging roles in cell and tissue polarity. *Trends Cell Biol*. 2008; 18: 199–209.
39. **Cocucci E, Racchetti G, Meldolesi J.** Shedding microvesicles: artefacts no more. *Trends Cell Biol*. 2009; 19: 43–51.
40. **Morel O, Toti F, Hugel B *et al.*** Cellular microparticles: a disseminated storage pool of bioactive vascular effectors. *Curr Opin Hematol*. 2004; 11: 156–64.
41. **Hutvagner G, Simard MJ.** Argonaute proteins key players in RNA silencing. *Nat Rev Mol Cell Biol*. 2008; 9: 22–32.
42. **Hunter MP, Ismail N, Zhang X *et al.*** Detection of microRNA expression in human peripheral blood microvesicles. *PLoS One*. 2008; 3: e3694.
43. **Yuan A, Farber EL, Rapoport AL *et al.*** Transfer of microRNAs by embryonic stem cell microvesicles. *PLoS One*. 2009; 4: e4722.